

On Bilateral Counterparty Credit Risk in Longevity-linked Security

by

Linghua Wei

A thesis submitted to
The Faculty of Graduate Studies of
The University of Manitoba
in partial fulfillment of the requirements
of the degree of

Master of Science

I.H. Asper School of Business
The University of Manitoba
Winnipeg, Manitoba, Canada
October 2017

© Copyright 2017 by Linghua Wei

Thesis advisor

Xuemiao Hao

Author

Linghua Wei

On Bilateral Counterparty Credit Risk in Longevity-linked Security

Abstract

In recent decades, longevity risk has become a common risk in life insurance industry. Longevity-linked securities are created to hedge such risk and traded over the counter. This thesis mainly focuses on evaluating the counterparty credit risk of longevity securities, using the newly proposed K-forward for example. Instead of only considering the counterparty credit risk from the hedger's perspective, we adopt bilateral credit value adjustment to evaluate the counterparty credit risk. The modelling consists of two significant parts. The first one is risk exposure estimated by locally linear Cairns–Blake–Dowd mortality model. The second part is joint default probability. We use a reduced-form default model to obtain the marginal risk-neutral term structure of default probability for the hedger and the hedge provider, and then employ the one-factor Gauss copula to describe the default correlation between the two parties. This work provides a framework to measure bilateral counterparty credit risk of longevity-linked securities.

Key words: BCVA, K-forward, LLCBD model, Longevity risk, Nelson–Siegel yield rate function, One-factor Gauss copula

Contents

Abstract	ii
Table of Contents	iii
Acknowledgments	iv
1 Introduction	1
2 Mortality Indexes	8
2.1 Mortality data	9
2.2 Two-factor CBD model	10
2.3 The LLCBD model	13
2.3.1 Hypothesis test on drift randomness	15
2.3.2 Estimation	17
2.3.3 Backtesting	19
3 Default probability	23
3.1 Marginal term structure of default probability	24
3.2 Calibration process	26
3.3 Copula model	35
4 BCVA of K-forward	37
4.1 Expected risk exposures EE^+ and EE^-	38
4.2 Numeric Results	39
5 Concluding remarks and future study	43
5.1 Thesis summary	43
5.2 Future Research	45
Bibliography	47

Acknowledgments

First of all, I would like to express my gratitude to my supervisor, Dr. Hao for the useful comments and engagement through the learning process of this master thesis. He is not only a rigorous scholar but also an excellent mentor. He gives me a chance to enter into actuarial area, and patiently imparts the actuarial knowledge. He leads me to improve my interdisciplinary and analytical thinking. Moreover, it is Dr. Hao who encourages me to be more confident to express my own ideas.

Secondly, I would like to thank my committee, Professors Jeffery Pai and Professor Alexander Paseka, for their insights, expertise, and support on the way. They provided some valuable suggestions on my research.

Finally, I must show my very profound gratitude to my parents and friends for providing me with unfailing support and continuous encouragement through my years of study and through the process of researching and writing this thesis. Especially, when I am upset, they always try to cheer me up and help me get out of dilemma.

This thesis would not have been possible without their supports and encouragement.

Chapter 1

Introduction

As a result of advances in medical technology, healthy life style and stable society, the mortality rate has declined in the recent years (Hari *et al.*, 2008). This kind of change influences the life insurance industry, especially pension funds and life annuity providers. They have to face longevity risk which is caused by the increasing life expectancy of the policy holders. The longer the life expectancy of the policy holders, the higher payout levels for the policy providers. The longevity risk not only comes from the reduction in mortality but also arises from the uncertain change rate of the mortality trend. Gallop (2006) finds the empirical evidence for mortality improvement pattern in the United Kingdom male during the previous decades. He points out that the average rate of mortality improvement is not constant and the improvement is quite rapid at the older age. Moreover, such mortality improvement trend also happens in other developed countries, such as Japan (Vaupel, 1997). To hedge the longevity risk and decrease the possible loss for the pension and life annuity providers, some mortality-linked and longevity-linked

securities, such as longevity bonds, q-forwards and K-forwards, are designed. This kind of financial derivatives is designed to reimburse the higher-than-expected payout via modelling and forecasting the future mortality rates with a stochastic mortality model. If there is a lower-than expected mortality rate, security holders will get cash inflows by participating in hedge process.

An emerging market, life market, has started to provide a platform for the transaction of longevity-linked securities (Blake *et al.*, 2013). However, it is not a mature market and the issue of longevity-linked securities still faces some problems, such as inadequate demand and counterparty credit risk. In the previous years, the public ignored the counterparty credit risk for the over-the-counter financial derivative, as the defaults are small probability events especially for large financial institutions. Thus, it is not necessary to evaluate such risk. It was not until 2008 financial crisis that the public were aware of the importance of incorporating the evaluation of counterparty credit risk into the financial derivatives pricing process. The market realized that even financial magnates, such as Lehman Brothers, have the possibility of bankruptcy. In the Basel II, the explicit definition of the counterparty credit risk is given as the risk that the counterparty could default before the maturity of the transaction. To regulate financial market, Basel III also provides detail stipulation on the counterparty credit risk calculation. Credit valuation adjustment (CVA) is one of the most popular method to obtain the market value of the counterparty credit risk. It is suggested to include the value of the counterparties credit risk, such as CVA, into the price of the over-the-counter securities.

CVA is usually regarded as unilateral credit valuation adjustment (UCVA), which just considers the default of the counterparty, while assumes that the institution own is default free. Bielecki and Rutkowski (2001) give a detail discussion and examples of UCVA. The general formula for the UCVA is expressed as

$$\text{UCVA} = (1 - R) \mathbb{E} \left[D(\tau) \cdot EE(\tau) \cdot 1_{(\tau \leq T)} \right], \quad (1.1)$$

where τ is the default time of the counterparty, $1 - R$ is the loss given default which measures the percentage of the risk exposure lost when the counterparty defaults, $D(\tau)$ is the discount factor at time τ which is implied from risk-free interest rates, $EE(\tau) = \mathbb{E}[E(\tau)]$ with $E(\tau)$ the risk exposure of the financial derivative at time τ , and $1_{(A)}$ denotes the indicator function of an event A . Note that since (1.1) is a pricing formula, the expectations in (1.1) should all be under a risk-neutral measure.

Although, UCVA is quite popular in recent years, Basel II realizes that instead of the default of only one particular party, both transaction participants are exposed to default risk. In this case, the counterparty risk possesses the bilateral nature. Actually, in real financial markets and with the experience of financial crisis, the bilateral assumption is more realistic (Brigo *et al.*, 2011). It is not credible to assume the existence of a “default-free” organization.

In contrast to UCVA, bilateral credit value adjustment (BCVA) evaluates the defaults from both sides under the assumption that both the institution and the counterparty may default before the final settlement. Considering the different default risks, Duffie and Huang (1996) use a switching discount rate to calculate

the present value of a financial derivative's cash outflow. Later work analyzes BCVA in more detail. For example, Brigo and Capponi (2008) point out that BCVA consists of two parts: CVA and debit valuation adjustment (DVA). The CVA part comes from the default of the counterparty, while the DVA part is due to the institution's own default. Thus, BCVA is the difference between CVA and DVA. The general formula of BCVA is

$$\begin{aligned} \text{BCVA} = & (1 - R_{\text{HP}}) \mathbb{E} \left[D(\tau_{\text{HP}}) \cdot EE^+(\tau_{\text{HP}}) \cdot 1_{(\tau_{\text{HP}} \leq T, \tau_{\text{H}} > T)} \right] \\ & - (1 - R_{\text{H}}) \mathbb{E} \left[D(\tau_{\text{H}}) \cdot EE^-(\tau_{\text{H}}) \cdot 1_{(\tau_{\text{H}} \leq T, \tau_{\text{HP}} > T)} \right], \end{aligned} \quad (1.2)$$

where HP and H respectively represent the counterparty (or the hedge provider) and the institution (or the hedger), $1 - R_{\bullet}$ is loss given default, τ_{\bullet} is default time, $EE^+(t) = \mathbb{E}[\max(E(t), 0)]$, and $EE^-(t) = -\mathbb{E}[\min(E(t), 0)]$. As in (1.1), all expectations in formula (1.2) should be under a risk-neutral measure. However, in this thesis we assume that mortality indexes are independent of financial market. As Cox and Pedersen (2000) explained for catastrophe risks, if a future cash flow depends only on mortality related variables, which are assumed independent of financial risk variables, then the cash flow's expectation under the risk-neutral measure coincides with that under the real-world measure. So we can calculate the expected risk exposures in (1.2) under the real-world measure.

We want to give more explanations to formula (1.2). The first part of the general BCVA formula is similar to the CVA calculation given in (1.1), but it is the joint probability density instead of the default probability of one specific counterparty. It is reasonable, because we consider the default of two participants and the

financial derivatives will terminate when the first default happens. Thus, we need to use the joint default probability which contains the default information of the two sides to calculate the first-to-default probability. In this part, we obtain the valuation of the counterparty credit risk based on the assumption that the hedge provider defaults while the hedge holder survives by the maturity. The second part of the general BCVA formula is the mirror image of the CVA, which is the DVA. Unlike the first part, it measures the possible “gains” when the hedge holder defaults. Therefore, there is a negative risk exposure instead of the positive one, because the default of hedge holder results in a loss to the hedge provider which may reduce the valuation of counterparty credit risk. Similarly, we use the joint default probability density to obtain the first-to-default probability based on the assumption that the hedge holder defaults while the hedge provider survives by the maturity. In this general formula, we include the correlation of the default events of the two parties. In other words, the defaults of two organizations are not only governed by company specific factor, but also governed by common factor. Moreover, in the general BCVA function, the indicator function is for the event that one party defaults before the maturity while the other survives until the maturity. The reason for this expression is that we need to include close-out risk. The payoff of the K-forward depends on the mortality indexes at maturity. Although one party defaults before the maturity, the other party may default between the first default time and maturity. Thus, the default of the other party could influence the settlement as the payoff is relied on the assumption that both parties should survive until the maturity. Based on this situation, we need to conduct adjustments

on the risk exposure to include the close-out risk.

In this paper, we take a simple longevity-linked security, K-forward, as an example to calculate and analyze the BCVA. K-forward is a zero-coupon swap first considered by Chan *et al.* (2014) and Tan *et al.* (2014). At the maturity date, the longevity risk hedger pays a predetermined proportion of floating (realized) mortality index, while the longevity risk hedge provider pays a predetermined proportion of the fixed mortality index. Thus, the actual settlement amount is the difference between the realized mortality index and the fixed mortality index. Figure 1.1 provides a brief relationship of the K-forward traders.

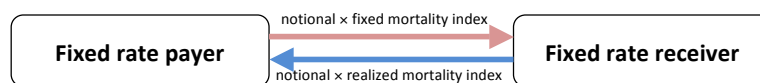


Figure 1.1: The transaction between two parties of a K-forward

The longevity-risk hedge mechanism of K-forward is derived from such difference between fixed mortality index and realized mortality index. For example, when the mortality index decreases and then results in a lower-than-expected mortality rate, the hedgers may face the longevity risk but they could obtain the reimbursement from the hedge providers. The positive payment from the hedge provider can cover the loss from the longevity risk. There are several advantages on the K-forward. The most important one is that the final payoff is derived from time-varying mortality index. Therefore, it is unnecessary to set a certain hedging age during the calculation, which could simplify the computation. Moreover, the implementation of K-forward is easier and more conducive (Chan *et al.* 2014), which will increase the liquidity. As a result of the introduction of K-forward, the di-

versification for the financial market will increase, which is a good signal for the market.

The rest of the thesis is organized as follows. In Chapter 2, we mainly discuss the mortality models with Canadian male population. We will compare the original two factor Cairns–Blake–Dowd (CBD) mortality model with the locally linear Cairns–Blake–Dowd (LLCBD) mortality model, and figure out the most suitable mortality model. With the chosen mortality model, we could forecast the future mortality indexes. In Chapter 3, we will use the bonds' market price to calibrate the reduced-form default model, Nelson-Siegel function, and get the marginal risk-neutral default probability. Then, it is possible to calculate the joint probability for two traders by combining marginal default probability with copula. With the mortality model and default model obtained in Chapters 2 and 3, we could calculate the BCVA in K-forwards in Chapter 4. Finally, Chapter 5 will give some conclusions and illustrate improvements could be done in the future research.

Chapter 2

Mortality Indexes

As mentioned in the previous part, the longevity-linked security, K-forward, could be used to hedge longevity risk. This kind of securities is traded over the counter. BCVA is used to evaluate the credit risk. There are two significant elements of the calculation of BCVA. One is the risk exposure, while the other is the default probability. In this chapter, we mainly focus on the risk exposure which can be obtained by mortality indexes with a certain CBD mortality model.

With the basic introduction on K-forward in Chapter 1, we could find that the payoff of the K-forward heavily depends on two different kinds of mortality indexes, the forward mortality indexes $\tilde{\kappa}_T^{(i)}$ and the realized mortality indexes $\kappa_T^{(i)}$. Specifically, stand at the point view of a fixed rate receiver, the settlement of the contract equals to an amount proportional to the difference between the fixed mortality indexes $\tilde{\kappa}_T^{(i)}$ and the realized mortality indexes $\kappa_T^{(i)}$ for a reference population

in a future reference year T . The formula can be shown in the following:

$$Y \cdot \left(\tilde{\kappa}_T^{(i)} - \kappa_T^{(i)} \right), \quad i \in \{1, 2\}, \quad (2.1)$$

where Y is the notional amount which is usually set as 1 dollar. In this paper, the payoff of K-forward could be considered as the risk exposure of BCVA.

Based on the above information, it is important to find out a proper CBD mortality model to obtain the realized and fixed mortality indexes. In this thesis, we mainly focus on comparison between two-factor CBD model and its extended model, LLCBD model. In the following sections, we give details of model selection and then conduct backtesting to confirm the selection.

2.1 Mortality data

The mortality data in this paper comes from Human Mortality Database (2017). We choose Canadian male aged from 50 to 89 as the reference population. The sample period is from 1941 to 2011 (71 years in total). Liu and Li (2016) show that there are three main reasons why it is reasonable to choose the age period [50,89]. First of all, the age period [50,89] is one of the most popular choices in the life insurance industry. This period is usually selected to fit the stochastic mortality models and applied to pension and annuity calculation. Thus, using this age range makes the estimation results more comparable and applicable. Secondly, it is found that, based on the Human mortality database guideline, the Canadian raw population counts are only reliable before age 89. In other words, raw population counts af-

ter age 89 are just estimations, instead of real population counts. Thus, when we fit a stochastic model, the population counts after age 89 may not be an authentic sample. Finally, beginning at age 50 removes the accident hump at the young ages for which the CBD/LLCBD mortality model can not fit such age effect structure. Moreover, with the age period after age 50, we could exclude the influence from the mortality improvement dynamics at the young ages.

2.2 Two-factor CBD model

In the previous literatures, some stochastic mortality models were raised. Most of these models have one or more time-varying parameters after being fitted to historical data. Based on the estimated mortality indexes, it is possible to forecast the future mortality rates of the reference population mortality. Chan *et al.* (2014) points out three important criteria when choosing a proper stochastic mortality model. First, instead of only showing the mortality improvement at overall level, mortality indexes should also demonstrate different age patterns of mortality changes. Secondly, mortality indexes should be straightforward. Thus, it is easy to transfer the contents to the public. Finally, mortality indexes should have new-data-invariant property. It means that historical values of $\kappa_t^{(i)}$ will not change even when new mortality data is included and the mortality model is updated accordingly.

Dowd *et al.* (2010) compares six widely used mortality models and stated briefly that the original two-factor CBD mortality model (Cairns *et al.*, 2006) is a relatively simple model with only two time-varying parameters $\kappa_t^{(1)}$ and $\kappa_t^{(2)}$, and it

possesses new-data-invariant property without adding any extra constraint. With two-factor CBD mortality model, one could obtain both the ex ante and ex post forecast. The original two-factor CBD model is demonstrated in the following:

$$y_{x,t} := \ln \left(\frac{q_{x,t}}{1 - q_{x,t}} \right) = \kappa_t^{(1)} + \kappa_t^{(2)}(x - \bar{x}) + \epsilon_{x,t}, \quad (2.2)$$

where $q_{x,t}$ is the crude probability that an individual at age x dies between time $t - 1$ and time t , \bar{x} is the average of the ages within the sample age range, $\epsilon_{x,t} \stackrel{\text{i.i.d.}}{\sim} N(0, \sigma_\epsilon^2)$ are sampling errors, and $\kappa_t^{(1)}$ and $\kappa_t^{(2)}$ are time-varying parameters that reflect the varying age effects on the mortality improvement. In particular, $\kappa_t^{(1)}$ demonstrates the level of the logit-transformed mortality curve. In other words, when there is a decreasing trend in $\kappa_t^{(1)}$, it means that there is a mortality improvement at overall level. Whereas, $\kappa_t^{(2)}$ represents the slope of the logit-transformed mortality curve, which implicates the age effects. For example, if $\kappa_t^{(2)}$ is positive, the improvement in mortality is larger at young age than that at the old age given the same condition.

After choosing the CBD model (2.2), we use the least squares method to estimate the historical values of $\kappa_t^{(1)}$ and $\kappa_t^{(2)}$. The results are shown in Figure 2.1. It is clearly seen in Figure 2.1 that the movements of indexes $\kappa_t^{(1)}$ and $\kappa_t^{(2)}$ are random. In particular, from 1941 to 2011, $\kappa_t^{(1)}$ always fluctuates around a downward trend while $\kappa_t^{(2)}$ first gradually moves downward for the first 40 years then increases in the next 15 years before a sharp drop.

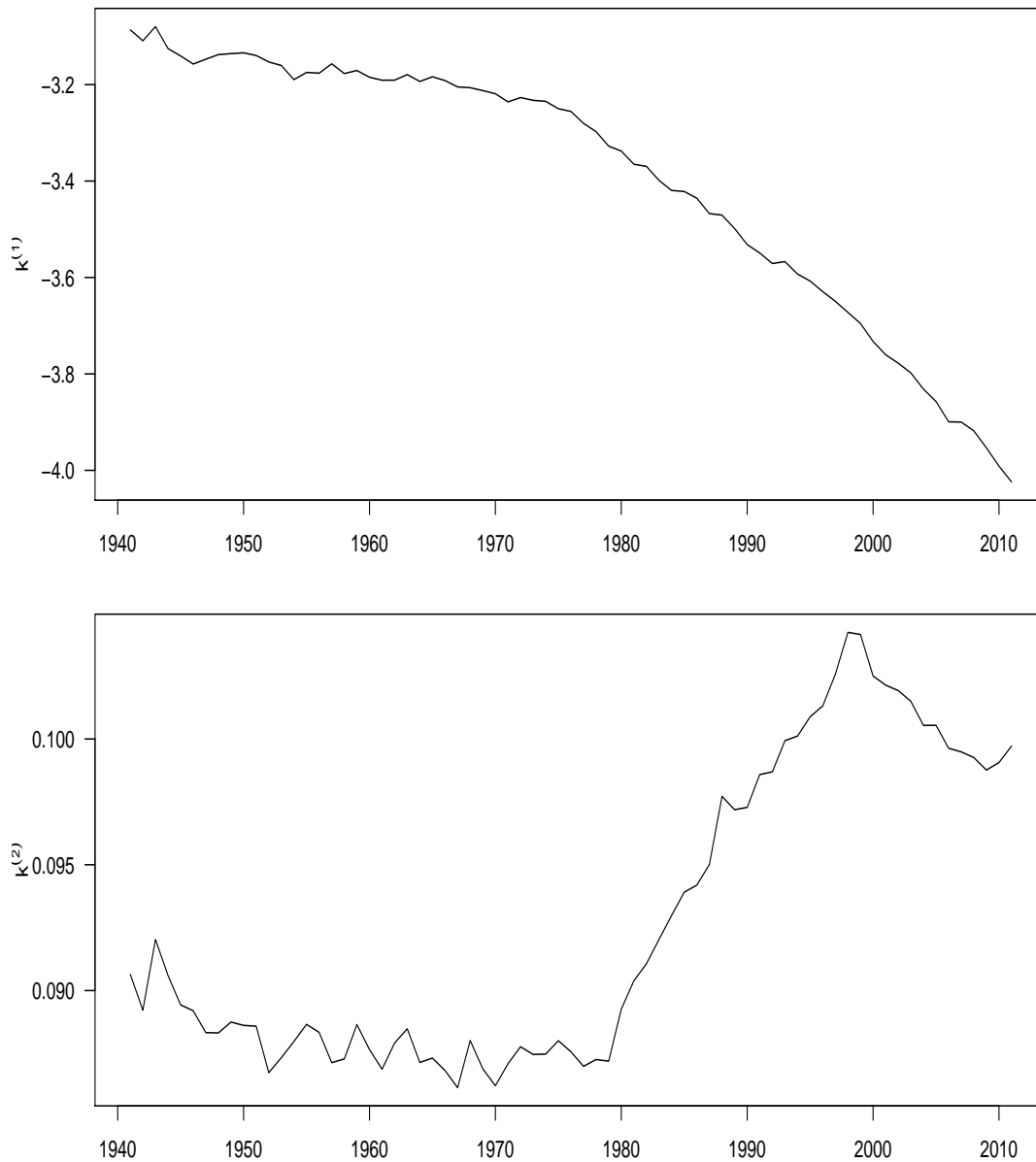


Figure 2.1: Historical values of $\kappa_t^{(1)}$ (upper panel) and $\kappa_t^{(2)}$ (lower panel) for Canada male population aged from 50 to 89, 1941–2011

Here we want to point out that the CBD mortality indexes have a unique feature called new-data-invariant property. In other words, after new mortality data is available and the CBD model (2.2) is updated accordingly, historical values of

$\kappa_t^{(i)}, i = 1, 2$, will not change. Based on this property, the concept of K-forward was proposed. See Chan *et al.* (2014) for more details.

2.3 The LLCBD model

In the original two-factor CBD mortality model, we assume that the bivariate random walk has constant drifts. If this assumption is reasonable, the estimated $\Delta\kappa_t^{(i)} = \kappa_t^{(i)} - \kappa_{t-1}^{(i)}$ should fluctuate around the sample means. The results of $\Delta\kappa_t^{(i)}$ are demonstrated in Figure 2.2. According to Figure 2.2, it seems that $\Delta\kappa_t^{(1)}$ does not fluctuate around the sample means. Instead, it has a decreasing trend. Therefore, we consider the following more general assumptions on stochastic $\kappa_t^{(1)}$ and $\kappa_t^{(2)}$. Supposed that $\kappa_t^{(i)}$, for $i = 1, 2$, are random walks with drift $C_t^{(i)}$, for $i = 1, 2$, which have stochastic nature. Then the equations can be expressed as:

$$\begin{cases} \Delta\kappa_t^{(i)} = C_{t-1}^{(i)} + \zeta_t^{(i)}, \\ C_t^{(i)} = C_{t-1}^{(i)} + v_t^{(i)}, \end{cases} \quad i = 1, 2, \quad (2.3)$$

where $t = t_0 + 1, t_0 + 2, \dots, t_1$. Here, t_0 is the beginning of sample period and t_1 is the ending of sample period. In the above formula, $\zeta_t^{(1)}, \zeta_t^{(2)}, v_t^{(1)}$ and $v_t^{(2)}$ are innovations which measure the uncertainty on mortality indexes. Suppose that, for each $i = 1, 2$, $\zeta_t^{(i)} \stackrel{\text{i.i.d.}}{\sim} N(0, \sigma_{\zeta^{(i)}}^2)$ and $v_t^{(i)} \stackrel{\text{i.i.d.}}{\sim} N(0, \sigma_{v^{(i)}}^2)$. Moreover, we assume that $\zeta_t^{(i)}$ and $v_t^{(j)}, i, j \in \{1, 2\}$, are mutually independent.

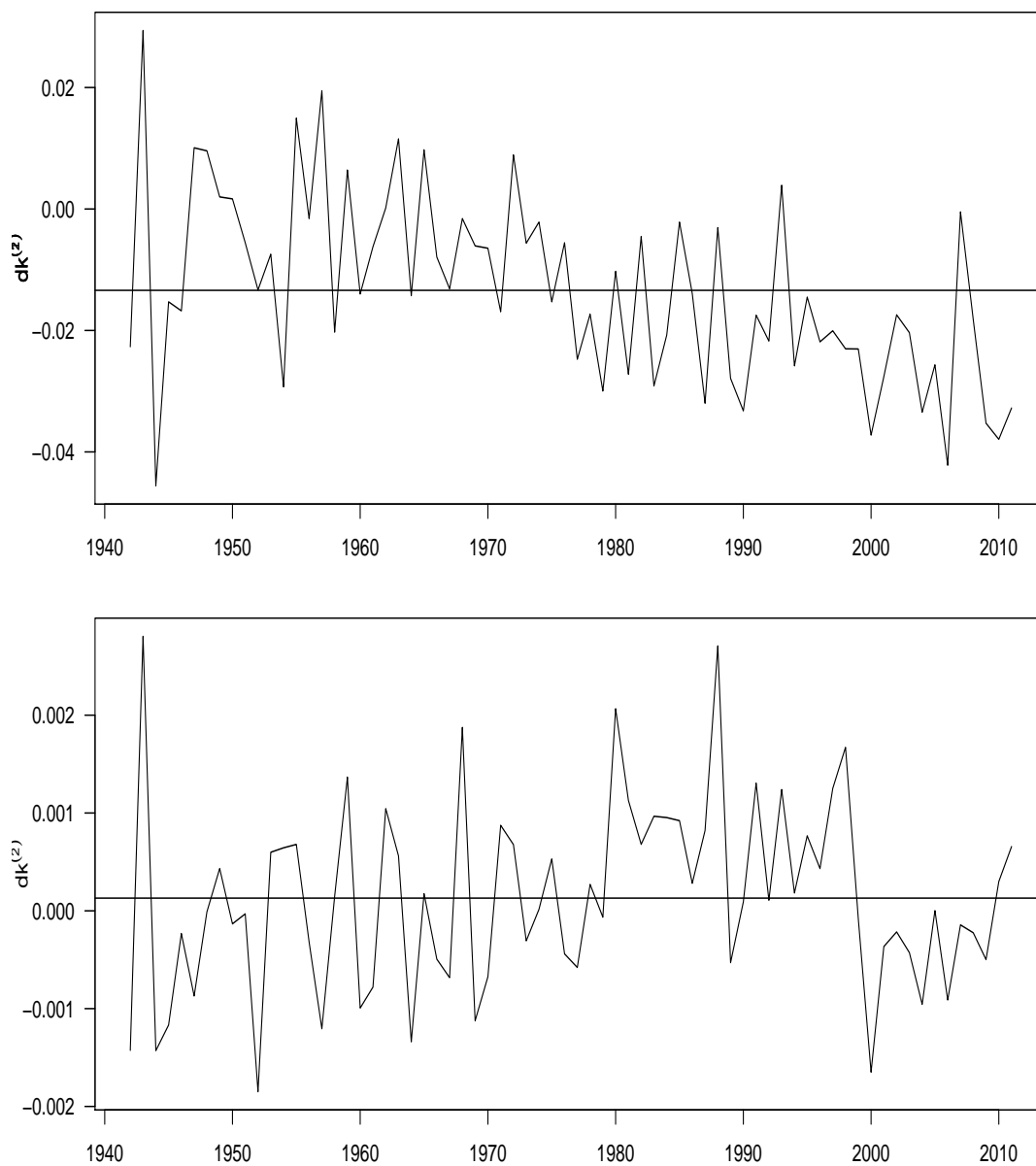


Figure 2.2: Historical values of $\Delta\kappa_t^{(1)}$ (upper panel) and $\Delta\kappa_t^{(2)}$ (lower panel) for Canada male population aged from 50 to 89, 1941–2011. The horizontal lines represent the sample means for $\Delta\kappa_t^{(1)}$ and $\Delta\kappa_t^{(2)}$, respectively.

2.3.1 Hypothesis test on drift randomness

To check stochastic nature of drifts, Liu and Li (2016) use a test called the locally most powerful invariant (LMPI) test, which was first proposed by Nyblom and Mäkeläinen (1983). In this statistical test, $H_0 : \sigma_{v^{(i)}}^2 / \sigma_{\xi^{(i)}}^2 = 0$ and $H_1 : \sigma_{v^{(i)}}^2 / \sigma_{\xi^{(i)}}^2 > 0$. If the statistic is greater than critical value, we will accept alternative hypothesis which means that $\sigma_{v^{(i)}}$ is not equal to 0 and thus the drift is not constant. Given the function provided by Liu and Li (2016), the null hypothesis statistic in LMPI test for $i = 1, 2$ is expressed as following:

$$L^{(i)} = \frac{\sum_{t=t_0+1}^{t_i} \left(\sum_{s=t}^{t_i} (\Delta\kappa^{(i)}(s) - \hat{C}^{(i)}) \right)^2}{\sum_{t=t_0+1}^{t_i} (\Delta\kappa^{(i)} - \hat{C}^{(i)})^2}, \quad (2.4)$$

where $\hat{C}^{(i)}$ is the sample mean. To obtain the final statistic, $L^{(i)}$ should be divided by $t_1 - t_0 - 1$. We could evaluate the stochastic nature of drifts via the comparison of statistics $L^{(i)} / (t_1 - t_0 - 1)$ and the rejection regions. After obtaining statistics, we need to calculate the reject regions. Nyblom and Mäkeläinen (1983) point out that $L^{(i)}$ has the same distribution as:

$$\frac{\sum_{k=1}^{t_1-t_0-1} \lambda_{k,t_1-t_0} (1 + \lambda_{k,t_1-t_0} \sigma_v^2 / \sigma_\xi^2) u_k^2}{\sum_{k=1}^{t_1-t_0-1} (1 + \lambda_{k,t_1-t_0} \sigma_v^2 / \sigma_\xi^2) u_k^2}, \quad (2.5)$$

where $\lambda_{k,t_1-t_0}^{-1} = 2(1 - \cos(\pi k / (t_1 - t_0)))$, $k = 1, 2, \dots, (t_1 - t_0 - 1)$, and $u_k \stackrel{\text{i.i.d.}}{\sim} N(0, 1)$. Thus, u_k^2 is a quadratic normal variable.

Considering (2.5), we could express the critical value c_α at significance level α

as

$$\alpha = \mathbb{P} \left(\frac{L^{(i)}}{t_1 - t_0 - 1} > c_\alpha \right) = \mathbb{P} \left(\sum_{k=1}^{t_1 - t_0 - 1} \left(\frac{\lambda_{k,t_1-t_0}}{t_1 - t_0 - 1} - c_\alpha \right) u_k^2 > 0 \right). \quad (2.6)$$

We need the value of c_α to decide whether $C_t^{(1)}$ is constant or not. Imhof (1961) showed that inverting the characteristic function could produce a general formula to obtain the quadratic forms for normal distribution. Accordingly, the probability in (2.6) can be written as

$$\mathbb{P}(V > 0) = \frac{1}{2} + \frac{1}{\pi} \int_0^\infty \frac{\sin \theta(y)}{y \rho(y)} dy, \quad (2.7)$$

with $\theta(y)$ and $\rho(y)$ given as

$$\theta(y) = \frac{1}{2} \sum_{k=1}^{t_1 - t_0 - 1} \tan^{-1}(\lambda_k y) \quad (2.8)$$

and

$$\rho(y) = \prod_{k=1}^{t_1 - t_0 - 1} (1 + \lambda_k^2 y^2)^{1/4}, \quad (2.9)$$

where $V = \sum_{k=1}^{t_1 - t_0 - 1} \lambda_k u_k^2$ and $\lambda_k = \frac{\lambda_{k,t_1-t_0}}{t_1 - t_0 - 1} - c_\alpha, k = 1, 2, \dots, t_1 - t_0 - 1$.

Then, we could conduct the LMPI test on Canada male population mortality data. Using (2.6)–(2.9), we get the critical value $c_\alpha = 0.4686$ when the significant level $\alpha = 0.05$. Meanwhile, with (2.4) we get the statistic values $L^{(i)} / (t_1 - t_0 - 1)$ for $\Delta \kappa_t^{(i)}, i = 1, 2$, respectively as 2.1446 and 0.3509. According to such results, we conclude that for Canadian male population drift $C_t^{(1)}$ is not a constant while drift $C^{(2)}$ is a constant.

2.3.2 Estimation

To facilitate the estimation process, let us first write the LLCBD model as a linear Gaussian state-space model. Denote by $\vec{y}_t = (y_{x_0,t}, y_{x_0+1,t}, \dots, y_{x_1,t})'$ the vector of observations at time t . Then we can rewrite models (2.2) and (2.3) as follows.

$$\begin{cases} \vec{y}_t = Z\vec{\alpha}_t + \vec{\epsilon}_t, \\ \vec{\alpha}_t = B\vec{\alpha}_{t-1} + \vec{\eta}_t, \end{cases} \quad (2.10)$$

where

$$Z = \begin{pmatrix} 1 & x_0 - \bar{x} & 0 & 0 \\ 1 & x_0 + 1 - \bar{x} & 0 & 0 \\ \vdots & \vdots & \vdots & \vdots \\ 1 & x_1 - \bar{x} & 0 & 0 \end{pmatrix}, \quad B = \begin{pmatrix} 1 & 0 & 1 & 0 \\ 0 & 1 & 0 & 1 \\ 0 & 0 & 1 & 0 \\ 0 & 0 & 0 & 1 \end{pmatrix},$$

$y_{x,t}$ is approximated by $m_{x,t}/(1 + 0.5m_{x,t})$, $\vec{\alpha}_t = (\kappa_t^{(1)}, \kappa_t^{(2)}, C_t^{(1)}, C_t^{(2)})'$, the vector of hidden states at time t , $\vec{\epsilon}_t = (\epsilon_{x_0,t}, \dots, \epsilon_{x_1,t})' \sim N(\vec{0}, \sigma_\epsilon^2 \mathbf{I}_{x_1-x_0+1})$ and $\vec{\eta}_t = (\zeta_t^{(1)}, \zeta_t^{(2)}, v_t^{(1)}, v_t^{(2)})' \sim N(\vec{0}, Q)$.

Depending on $\vec{\alpha}_t$, the log-likelihood function can be written as

$$\begin{aligned} \ln(\mathcal{L}) = & -\frac{1}{2\sigma_\epsilon^2} \sum_{t=t_0}^{t_1} (\vec{y}_t - Z\vec{\alpha}_t)' (\vec{y}_t - Z\vec{\alpha}_t) - \frac{(t_1 - t_0 + 1)(x_1 - x_0 + 1)}{2} \ln(\sigma_\epsilon^2) \\ & - \frac{1}{2} \sum_{t=t_0+1}^{t_1} (\vec{\alpha}_t - B\vec{\alpha}_{t-1})' Q^{-1} (\vec{\alpha}_t - B\vec{\alpha}_{t-1}) - \frac{1}{2} \sum_{t=t_0+1}^{t_1} \ln|Q| + c_l. \end{aligned} \quad (2.11)$$

Then Expectation-Maximization (EM) algorithm can be used to acquire the maximum likelihood estimations for σ_ϵ and the parameters in Q . See, for instance, Holmes (2013).

Based on the LMPI test result, only $C_t^{(1)}$ follows a random walk. There are total 6 parameters and 3 hidden states. The LLCBD model can be simplified as:

$$\begin{cases} \vec{y}_t = Z\vec{\alpha}_t^* + \vec{\epsilon}_t, \\ \vec{\alpha}_t^* = B\vec{\alpha}_{t-1}^* + \vec{u} + \vec{\eta}_t^*, \end{cases} \quad (2.12)$$

where

$$Z = \begin{pmatrix} 1 & x_0 - \bar{x} & 0 \\ 1 & x_0 + 1 - \bar{x} & 0 \\ \vdots & \vdots & \vdots \\ 1 & x_1 - \bar{x} & 0 \end{pmatrix}, \quad B = \begin{pmatrix} 1 & 0 & 1 \\ 0 & 1 & 0 \\ 0 & 0 & 1 \end{pmatrix},$$

$\vec{\alpha}_t^* = (\kappa_t^{(1)}, \kappa_t^{(2)}, C_t^{(1)})'$, the vector of hidden states at time t , $\vec{\epsilon}_t = (\epsilon_{x_0,t}, \dots, \epsilon_{x_1,t})' \sim N(\vec{0}, \sigma_\epsilon^2 \mathbf{I}_{x_1-x_0+1})$, $\vec{u} = (0, C^{(2)}, 0)'$ and $\vec{\eta}_t^* = (\zeta_t^{(1)}, \zeta_t^{(2)}, v_t^{(1)})' \sim N(\vec{0}, Q^*)$.

Moreover, we could also obtain the original CBD model by setting $\vec{\eta}_t^{**} = (\tilde{\zeta}_t^{(1)}, \tilde{\zeta}_t^{(2)})' \sim N(\vec{0}, Q^{**})$. In the original CBD model, there are 2 hidden state space and 6 parameters.

We use the mortality data of Canadian males aged 50 to 89 from 1941 to 2011 to fit the original CBD and the LLCBD model. The estimation results for unknown parameters are shown in Tables 2.1 and 2.2, respectively.

It is shown that the estimation and standard error for σ_ϵ^2 are almost the same in two models. The main difference appears in the covariance matrix Q . We found that there is an obvious reduction in the variance of $\kappa_t^{(1)}$, while there is a relatively small decrease in the variance of $\kappa_t^{(2)}$. The reason is that some volatilities of $\Delta\kappa_t^{(1)}$ are captured by $C_t^{(1)}$.

Parameter	Estimate	Standard error
σ_ϵ^2	$2.31e^{-3}$	$6.48e^{-4}$
$C^{(1)}$	$-1.33e^{-2}$	$1.51e^{-3}$
$C^{(2)}$	$1.32e^{-4}$	NA
$Q_{1,1}^{**}$	$2.02e^{-4}$	$1.47e^{-3}$
$Q_{2,1}^{**}$	$1.83e^{-8}$	NA
$Q_{2,2}^{**}$	$6.19e^{-7}$	$9.59e^{-5}$
AIC = -8938.12 Log-likelihood = 4475.06		

Table 2.1: The estimate value and standard error for σ_ϵ^2 and Q^{**} in the original CBD

Parameter	Estimate	Standard error
σ_ϵ^2	$2.31e^{-3}$	$6.50e^{-4}$
$C^{(2)}$	$1.29e^{-4}$	$1.05e^{-4}$
$Q_{1,1}^*$	$6.27e^{-5}$	$1.65e^{-3}$
$Q_{2,1}^*$	$2.99e^{-6}$	$2.65e^{-4}$
$Q_{2,2}^*$	$6.50e^{-7}$	$1.14e^{-4}$
$Q_{3,3}^*$	$5.08e^{-6}$	$9.51e^{-4}$
AIC = -8956.843 Log-likelihood = 4484.422		

Table 2.2: The estimate value and standard error for σ_ϵ^2 and Q^* in the LLCBD

Comparing the AIC and log-likelihood in two different CBD model, we found that LLCBD has a lower AIC and higher Log-likelihood which indicates a better fitting results. Thus, LLCBD model is better than the original CBD model when we fit the Canadian male mortality model.

2.3.3 Backtesting

After fitting the mortality model, it is necessary to evaluate the accuracy of the forecasts within a certain time horizon. Dowd *et al.* (2010) raise a backtesting framework which could be applied to multiperiod-ahead forecast of the stochastic mortality models. They conducted the backtests for CBD models (M1–M7) to eval-

uate the out-of-sample forecasting performance. In the following parts, we first use the Canadian male mortality data from 1941 to 1991 to fit the original CBD model and the LLCBD model. Then, we use the estimated parameters to conduct the simulation and obtain the confidence interval and median value for the forecasted $\kappa_t^{(1)}$ and $\kappa_t^{(2)}$ from 1992 to 2011 in both mortality models. Finally, we evaluate the consistence of the actual κ_t and forecasted results. The backtesting results of the original CBD model are shown in the figure 2.3, while the results of the LLCBD are demonstrated in figure 2.4.

Comparing figure 2.3 and figure 2.4, we found that these two models produce the same forecasting performance in $\kappa_t^{(2)}$. Only a small part of the actual $\kappa_t^{(2)}$ out of the range. In contrast, the forecasting performance is different in $\kappa_t^{(1)}$ for these two models. In the LLCBD model, the actual $\kappa_t^{(1)}$ lies within the confidence interval in all predicting period, while in the original model most parts of the actual $\kappa_t^{(1)}$ are outside of the confidence interval. The actual $\kappa_t^{(1)}$ lies beyond the lower bound of the confidence interval in the original CBD model, which may result in lower risk exposure. According to the backtesting results, it is indicated that the LLCBD model performs better in the forecasting process. The calculation of BCVA could be significantly affected by the prediction of the future mortality indexes. Thus, in the rest of the paper, we choose the LLCBD model to calculate the risk exposures.

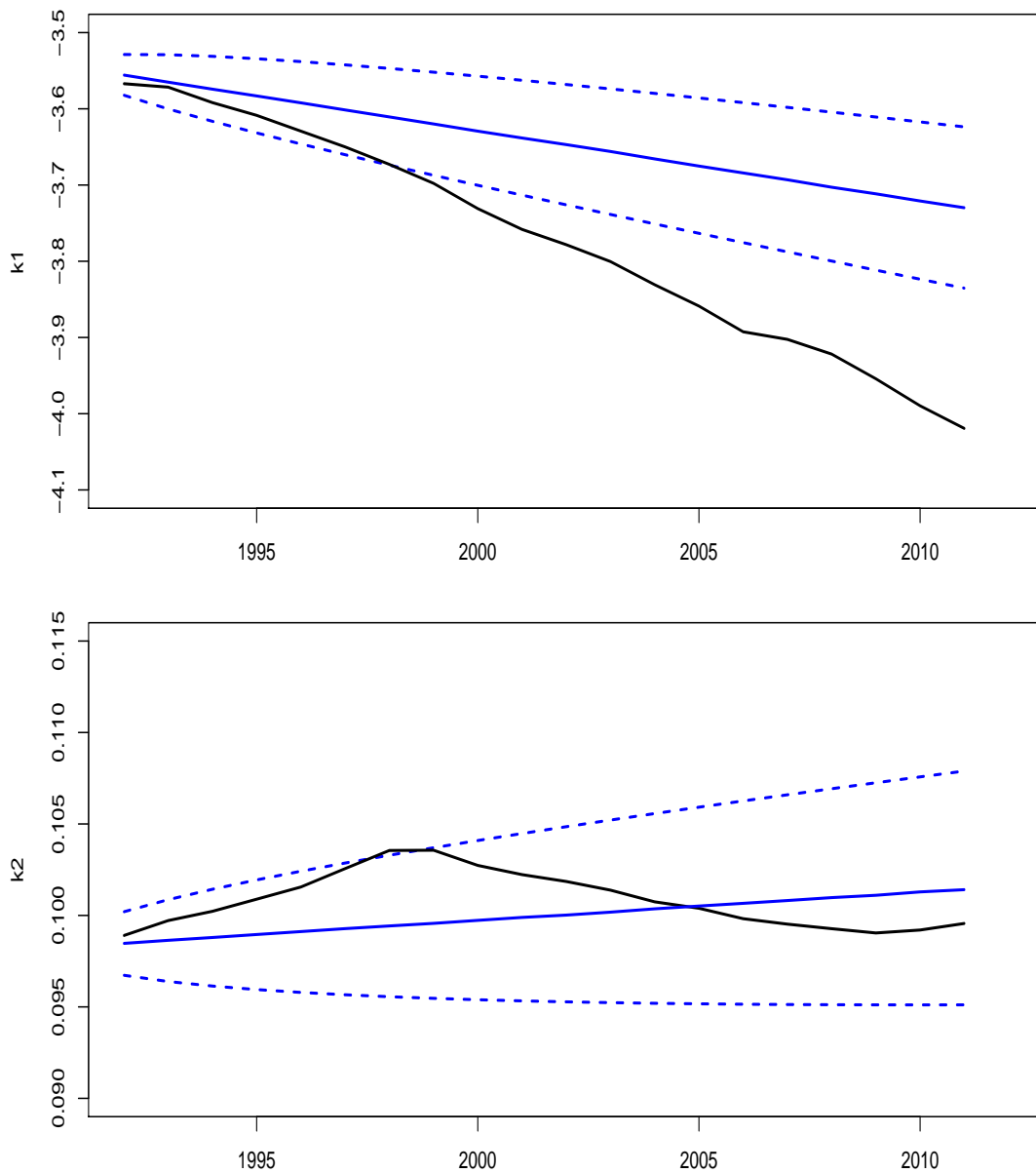


Figure 2.3: The 95% confidence interval and median line of the forecasting $\kappa_t^{(1)}$ (upper panel) and $\kappa_t^{(2)}$ (lower panel) for 1992-2011 with the original CBD model. The model is fitted with the Canadian male mortality data from 1941 to 1991. The blue dashed line is the lower and upper bounds of the confidence interval, the blue solid line represents the median line, and the black solid line is the real outcomes of the mortality indexes.

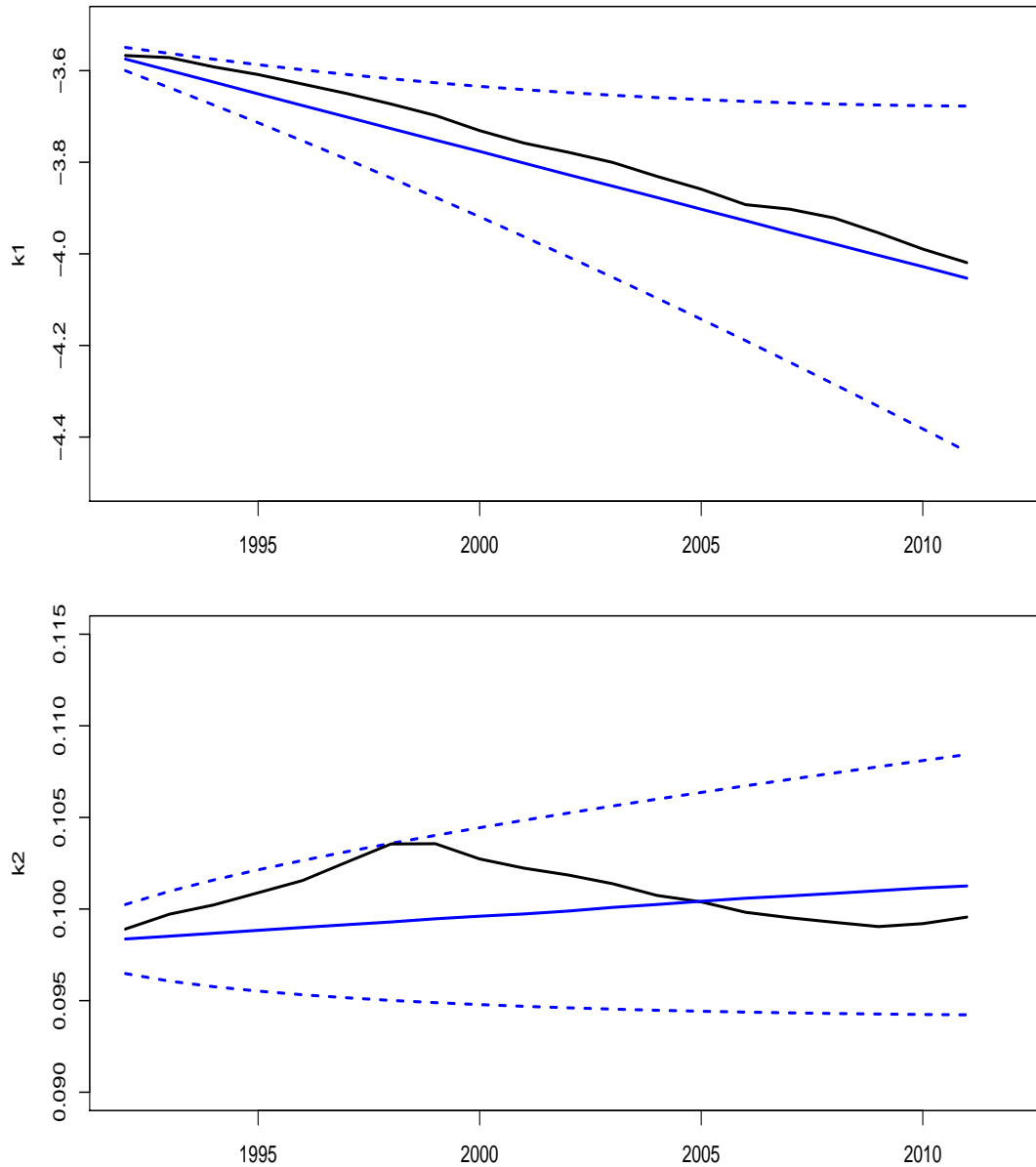


Figure 2.4: The 95% confidence interval and median line of the forecasting $\kappa_t^{(1)}$ (upper panel) and $\kappa_t^{(2)}$ (lower panel) for 1992-2011 with the LLCBD model. The model is fitted with the Canadian male mortality data from 1941 to 1991. The blue dashed line is the lower and upper bounds of the confidence interval, the blue solid line represents the median line, and the black solid line is the real outcomes of the mortality indexes.

Chapter 3

Default probability

In the last chapter, we have already discussed the selection of the mortality model and chosen LLCBD model to forecast the mortality indexes. In this section, we mainly focus on the risk-neutral default probability which is another important issue of the BCVA calculation. There are two main methods to model the default probability, the structural approach and the reduced-form approach. The structural form model is first introduced by Merton (1974). In the structural model, the default is modelled as the default-triggering process. For example, the default happens when the firm's value modelled by a stochastic process first drops below the low boundary (Hao *et al.*, 2013). In 1995, Jarrow and Turnbull first used the reduced-form model to price the financial derivatives with default risks. Unlike the default in the structural approach, the default in the reduced-form model is considered as an unexpected process. And the intensity process is used to modeling the default probability. Compared with structural approach, this method simplify the whole valuation process. Given the definition, the structural model

relies on the accounting reports, but in reality there exists noise in the accounting information which may cause valuation errors. Compared with the structural model, the reduced-form model are consistent with asymmetric equilibrium prices (Jarrow, 2011). Therefore, in this part, we use the reduced-form model to obtain the default probability for hedger and hedge provider. The survival probability is expressed as:

$$S(t) = \exp \left(- \int_0^t h(s) ds \right), \quad (3.1)$$

where $h(s)$ is the hazard rate.

3.1 Marginal term structure of default probability

It is often assumed that hazard rate is constant or piece-wise constant over time, which simplifies the calculation. However, this assumption may result in model errors. Instead of a piece-wise constant hazard rate, Nelson-Siegel model has a time-varying intensity $h(t)$. It is more sophisticated, because the intensity includes the structure effects (Bluhm *at al.*, 2010). The Nelson-Siegel model is first introduced by Nelson and Siegel (1987) to price long-term Treasury bonds, because this model could successfully fit different shapes of the yield curve. Additionally, this model could also efficiently smooth the parameters, which implies that with fewer parameters one could obtain the intensity without material deterioration in the prediction accuracy. The Nelson-Siegel hazard rate, $h(t)$, is given by:

$$h(t; \boldsymbol{\beta}) = \beta_0 + \beta_1 e^{-t/\beta_3} + \beta_2 e^{-t/\beta_3} t / \beta_3. \quad (3.2)$$

Based on the $h(t; \boldsymbol{\beta})$, the cumulative hazard rate is expressed as:

$$H(t; \boldsymbol{\beta}) = \frac{1}{t} \int_0^t h(s; \boldsymbol{\beta}) ds = \beta_0 + (\beta_1 + \beta_2)(1 - e^{-t/\beta_3})\beta_3/t - \beta_2 e^{-t/\beta_3}. \quad (3.3)$$

For equations (3.2) and (3.3), $t > 0$, because time t must be positive, and $\boldsymbol{\beta} = (\beta_0, \beta_1, \beta_2, \beta_3)^\top \in \mathbb{R}^4$. As Nelson-Siegel model is a parsimonious model, every parameter of $\boldsymbol{\beta}$ has economic meaning. For example, β_0 represents the long-term converging value of the default intensity. In other words, when time t goes infinitely the default intensity approaches β_0 . Moreover, as the default intensity should always be positive when the bonds are defaultable, β_0 should be larger than 0. Additionally, β_1 is the short-term effect on the default intensity which describes the short-term deviation from the mean. It could be positive or negative, when $\beta_1 > 0$, there is a downward sloping term structure. On the contrary, if $\beta_1 < 0$, the default intensity is upward sloping. As for β_2 , it is the medium-term effects on the default intensity and captures the humps when it does not equal 0. As for the last parameter, β_3 , it is the time scalar parameter.

Using (3.1)–(3.3), we could get the survival probability as:

$$S(t; \boldsymbol{\beta}) = \exp(-tH(t; \boldsymbol{\beta})), \quad t \geq 0. \quad (3.4)$$

Considering that $S(t; \boldsymbol{\beta})$ is the survival probability of the hedger and hedge providers, it must meet some criteria. First of all, $S(t; \boldsymbol{\beta})$ should be a monotone decreasing

function which means that $S'(t; \beta) < 0$ for all $t \geq 0$. Specifically, at time 0, given β , $S(t; \beta) = 1$, while as time goes infinitely, $\lim_{t \rightarrow \infty} S(t; \beta) = 0$. To meet these properties, there are additional constraints on the parameters (β) which are demonstrated in the following:

(C1) $\beta_0 > 0$;

(C2) $\beta_0 + \beta_1 > 0$;

(C3) $\beta_2 > \beta_l$ with β_l uniquely satisfying $\beta_l < \beta_1$ and $\beta_0 + \beta_l \exp(\beta_1/\beta_l - 1) = 0$.

See Hao *et al.* (2017) for more details.

3.2 Calibration process

Having decided on the default probability model, we could estimate the parameters from the bonds' market information. In this thesis, without considering the call policy, we only collect the non-callable bonds market prices from the secondary market. In the secondary market, the bonds' market price is also called "dirty price" which consists of "clean price" and accrued interest. Not only does it reflect the issuers' credit quality but also the interest accruing. In this section, we match the "dirty price", which is derived from the reduced-form model, with its corresponding market price. To obtain the "dirty price", we need to collect a set of bonds' market information, including maturity, principal, coupon rate and so on, on the same date. For each hedger or hedge provider, we collect more than five non-callable bonds to ensure the accuracy of calibration results. Considering that "dirty price" is the present value of the future cash flows, it is also necessary

to obtain discount factor derived from the risk-free rate. We choose the US Treasury continuously zero yield rate on the same date as the risk-free rate, because the bonds used in this thesis are all measured in US dollars and we want to make a consistency. Based on the financial market information, the "dirty price" for a specific bond is expressed as:

$$\sum_{j=1}^n DF(s_j) \cdot c\Delta_j \cdot S(s_j) + V \cdot DF(s_n) \cdot S(s_n) + V \cdot R \cdot \int_0^{s_n} DF(s)F(ds). \quad (3.5)$$

Formula (3.5) is the summation of the discounted future coupon and principal payments with the consideration of credit risk. In this formula, $s_j, j = 1, \dots, n$, are the coupon payment moments and s_n is the maturity, c is the bond coupon rate, Δ_j is the fraction of years between s_{j-1} and s_j , V is the par value (usually \$100), R is the recovery rate, $DF(\cdot)$ is the risk-free discount factor, $S(\cdot) = S(\cdot; \beta)$ for simplicity, and $F(\cdot) = 1 - S(\cdot)$. Note that formula (3.5) is derived under the conditions that, at the default time, recovery amount is a percentage of the par value and the recovery rate is constant at 37% over time. The idea of constant recovery rate comes from the Chapter 24 of Hull (2014). Hull provides a table containing average recovery rate for bonds in different credit classes. In this paper, most of the bonds come from senior unsecured class. Thus, the corresponding average recovery rate is 37%. To simplify the calculation, we set the recovery rate to be 37%, a constant.

To find the optimal default intensity function, we need to find a set of optimal parameters under constraints C1 to C3, producing a minimum absolute difference between dirty price and corresponding market price. Such parameters β are ex-

pressed as:

$$\beta^* = \arg \min_{\beta} \frac{1}{K} \sum_{k=1}^K |\text{dirty price}_k - \text{market price}_k|, \quad (3.6)$$

where dirty prices are derived from (3.5) and market prices are collected from Bloomberg. According to the calibration process, we are able to obtain a set of parameters β^* which produces a best match between "dirty price" and market price.

In the process of calibration, JP Morgan is chosen as the hedge provider, and New York Life and Prudential Financial are selected as two different the hedgers. These three institutions have already participated in the longevity-linked securities in the past years. So they are the potential traders of K-forward. We collect a set of bonds information, containing maturity, par value, coupon, coupon payment frequency and market value, for the hedger and hedge providers from Bloomberg database on November 7, 2016. There are 6 bonds for JP Morgan, 7 bonds for New York Life and 7 bonds for Prudential Financial. The detailed information is illustrated in Tables 3.1 - 3.3:

Combining (3.5) and (3.6), we find that the parameters appear in the exponent. Therefore, we need to implement nonlinear optimization instead of linear optimization. The calibration is conducted in R 3.3.1 with NLOpt package.

Table 3.1: Six bonds of JP Morgan on November 7, 2016

Maturity	Par	Coupon	Frequency	Last price	Currency	Type
1.216	100.000	1.800	semiannually	100.470	USD	Senior secured
2.956	100.000	2.200	semiannually	101.394	USD	Senior secured
4.773	100.000	4.350	semiannually	109.394	USD	Senior secured
5.879	100.000	3.250	semiannually	104.158	USD	Senior secured
21.532	100.000	6.400	semiannually	134.465	USD	Senior secured
24.701	100.000	5.600	semiannually	124.505	USD	Senior secured

Table 3.2: Seven bonds of New York Life on November 7, 2016

Maturity	Par	Coupon	Frequency	Last price	Currency	Type
0.518	100.000	1.650	semiannually	100.365	USD	Senior secured
1.469	100.000	1.300	semiannually	101.068	USD	Senior secured
2.611	100.000	2.150	semiannually	101.865	USD	Senior secured
3.263	100.000	1.950	semiannually	100.796	USD	Senior secured
9.688	100.000	2.350	semiannually	97.603	USD	Senior secured
16.523	100.000	5.875	semiannually	120.264	USD	Senior secured
23.036	100.000	6.75	semiannually	137.872	USD	Senior secured

Table 3.3: Seven bonds of Prudential Financial on November 7, 2016

Maturity	Par	Coupon	Frequency	Last price	Currency	Type
1.770	100.000	2.300	semiannually	101.353	USD	Senior secured
4.025	100.000	4.500	semiannually	109.314	USD	Senior secured
7.523	100.000	3.500	semiannually	105.067	USD	Senior secured
12.945	100.000	3.850	semiannually	99.928	USD	Senior secured
16.696	100.000	5.750	semiannually	118.454	USD	Senior secured
20.115	100.000	5.700	semiannually	119.738	USD	Senior secured
25.041	100.000	6.800	semiannually	121.649	USD	Senior secured

The calibration results are shown in Figures 3.1–3.3. The blue bars in each figure represent the selected bonds' market prices, while the red bars show the corre-

sponding "dirty price" derived from (3.5).

The comparison of market prices and calibrated prices for JP Morgan is demonstrated in Figure 3.1. The mean absolute error is 0.27277 for six JP Morgan bonds. The optimal parameters are $\beta_{\text{JPM}}^* = (1.86956e^{-6}, 0.00054, 0.05903, 5.90509)^T$. The absolute percentage error ranges from $1.423e^{-6}$ to 0.024. It means that the largest discrepancy between "dirty price" and market price is no more than 2.4% of the market price for six selected JP Morgan bonds.

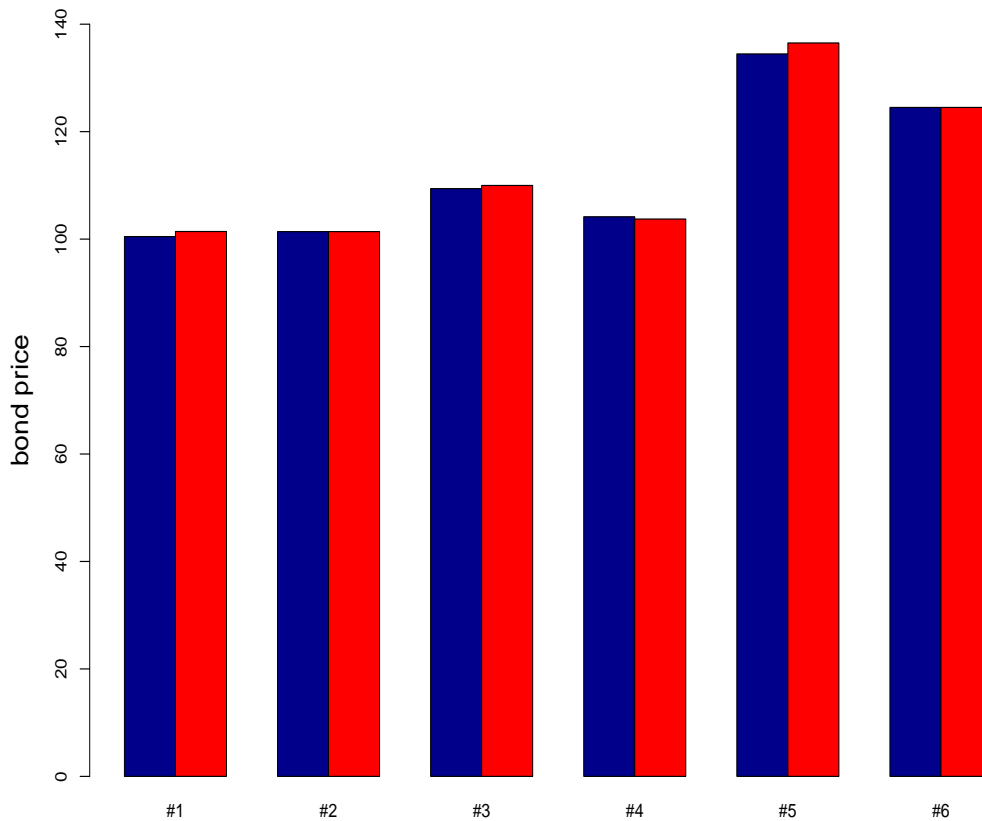


Figure 3.1: Calibration results for JP Morgan. The blue bars represent bonds' market prices and the red bars represent bonds' dirty prices with $\beta_{\text{JPM}}^* = (1.86956e^{-6}, 0.00054, 0.05903, 5.90509)^T$. The mean absolute error is 0.27277.

For New York Life, the comparison of the market prices and "dirty prices" is illustrated in Figure 3.2. The mean absolute error is 1.27 with the optimal parameters $\beta_{\text{NYL}}^* = (1.0e^{-8}, 0.00395, 0.05200, 7.18440)^\top$. The scope of absolute percentage error is $[1.738e^{-8}, 0.033]$. For all seven bonds, the difference between "dirty price" and "market price" is no more than the 3.3% of the corresponding market price.

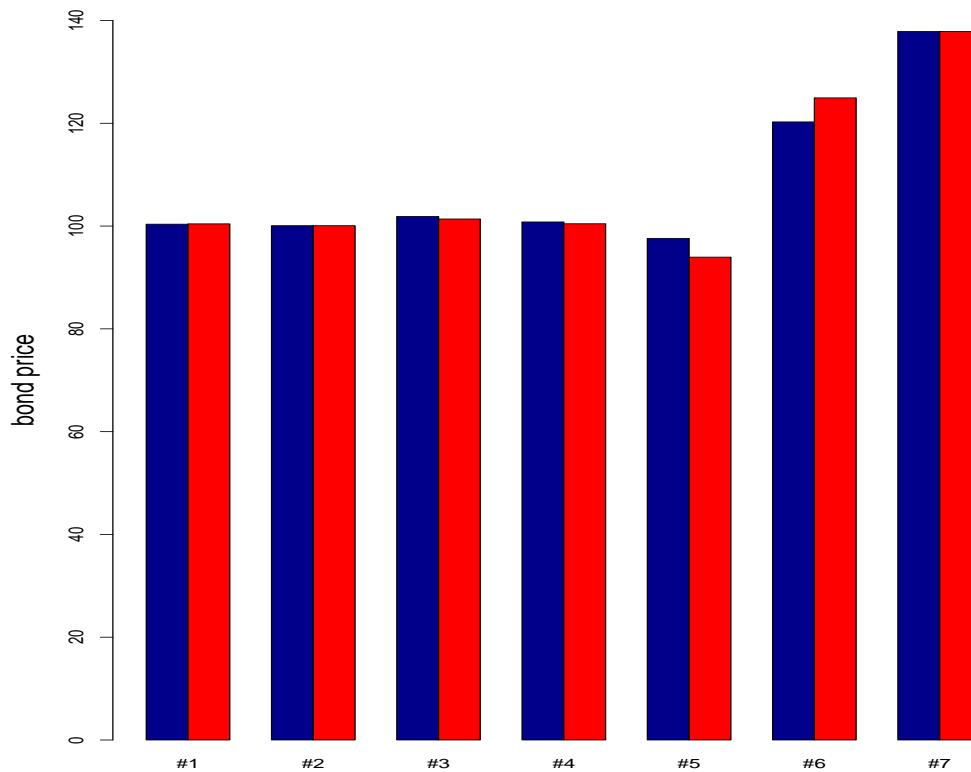


Figure 3.2: Calibration results for New York Life. The blue bars represent bonds' market prices and the red bars represent bonds' dirty prices with $\beta_{\text{NYL}}^* = (1.0e^{-8}, 0.00395, 0.05200, 7.18440)^\top$. The mean absolute error is 1.26997.

According to the calibration process, the mean absolute error for seven Prudential Financial bonds is 0.448 and comparison result is shown in Figure 3.3. The optimal parameters in this condition are $\beta_{\text{PF}}^* = (6.08092e^{-8}, 0.00970, 0.05731, 6.48221)^\top$.

The scope of absolute percentage error is from $6.121e^{-14}$ to 0.021. It indicates that, for all seven bonds, the difference between "dirty price" and "market price" is no more than the 2.1% of the corresponding market price.

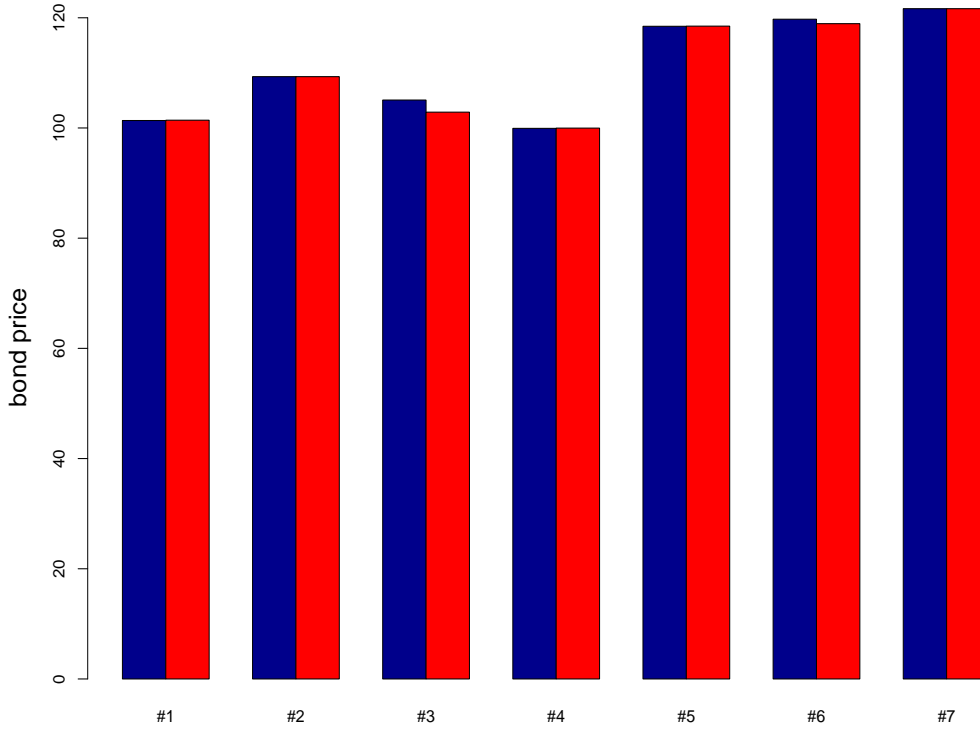


Figure 3.3: Calibration results for Prudential Financial. The blue bars represent bonds' market prices and the red bars represent bonds' dirty prices with $\beta_{PF}^* = (6.08092e^{-8}, 0.00970, 0.05731, 6.48221)^T$. The mean absolute error is 0.44800.

Knowing the optimized parameters β^* for three potential traders, we could also obtain the credit spread curves. In this thesis, the credit spread can be simplified as:

$$CS = (1 - R)H(t; \beta), \quad (3.7)$$

where R is the recovery rate for the potential traders, $H(t; \beta)$ is the cumulative hazard rate in (3.3). Based on this general formula for credit spread and calibration results, we plot the credit spread curves for JP Morgan, New York Life and Prudential Financial. The figures are shown in the following:

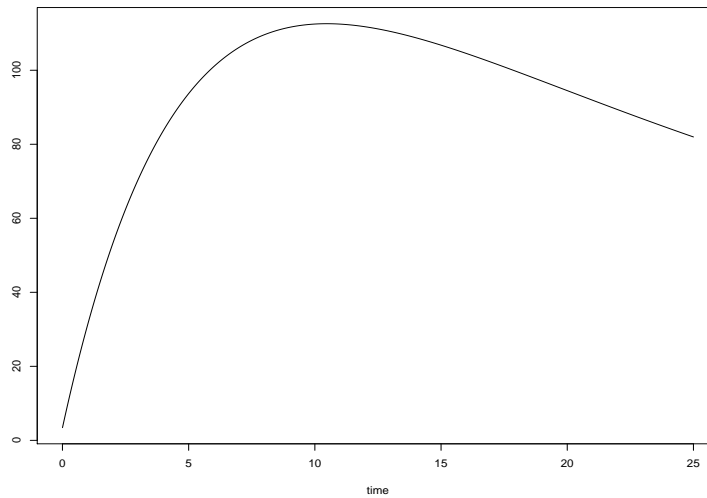


Figure 3.4: Credit spread curve for JP Morgan.

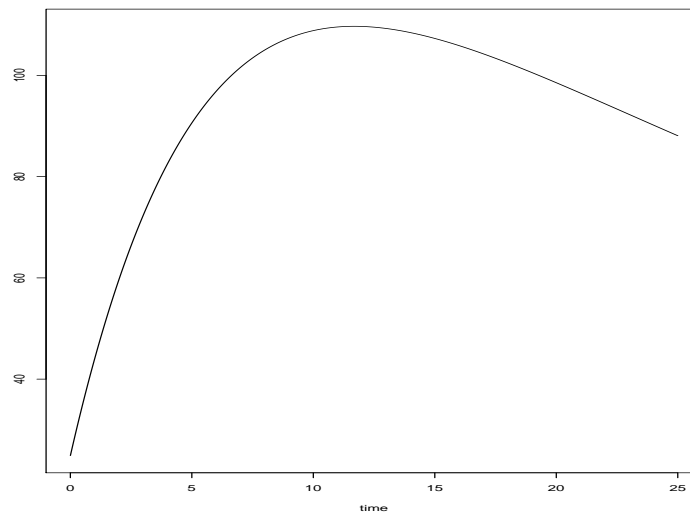


Figure 3.5: Credit spread curve for New York Life.

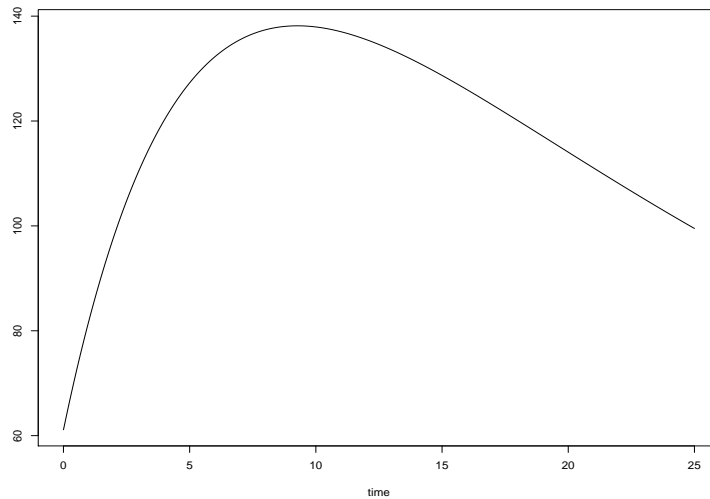


Figure 3.6: Credit spread curve for Prudential Financial.

From Figures 3.4–3.6, we find that the credit spread curves for three traders are all hump shaped, which is the general B-rating credit spread curve (Lando and Mortensen, 2005). All of them first increase to the highest point and then start decreasing gradually. Although they have the same shapes, there are still some differences. For example the highest points for three traders are different. The credit spread of JP peaks around 120 bps, while that of New York Life and of Prudential Financial is close to 110 bps and 140 bps, respectively. In addition, for JP Morgan, it reaches the highest credit spread around 10 years. But for New York Life and Prudential Financial, the first one arrives the peak after 10 years, while the other before 10 years. These slight differences may come from the different credit rating. In Moody's, all bonds of JP Morgan and New York Life come from A-rating, while the bonds of Prudential Financial are in the position of B-rating. However, on the whole, all risk neutral credit spread curves perform like B-rating curves

and there is no huge discrepancy between two different credit rating levels. This phenomenon reflects the risk aversion nature of the financial market, especially when the market evaluates the credit risk.

3.3 Copula model

In this thesis, we focus on BCVA which considers default risk from two participants and includes joint default probability instead of marginal default probability. These two traders are all in financial industry and they are not completely independent of each other. Usually, we use copula to construct joint distribution, because copula not only describes the marginal behaviour of individual risk but also demonstrates the dependence structure of all participants.

We assume that the dependence between the default times of the hedger and the hedge provider is governed by a one-factor Gauss copula. The assumption is that:

$$X_i = \sqrt{\rho_i}V + \sqrt{1 - \rho_i}\zeta_i, \quad (3.8)$$

where $i \in \{H, HP\}$, $\rho_i \in (0, 1)$, and V and ζ_i are iid standard normal random variables and independent of each other. Specifically, V is a common factor which affects all companies in the transaction, while ζ_i is a factor which only affect company i . When $\rho_H = \rho_{HP} = 0$, the defaults of the hedger and the hedge provider are completely independent and are only controlled by ζ_H and ζ_{HP} , respectively. On the contrary, when $\rho_H = \rho_{HP} = 1$, the defaults are completely dependent and controlled by common factor V . It is obvious that $\mathbf{X} = (X_H, X_{HP})' \sim N_2(\mathbf{0}, P)$,

where

$$P = \begin{pmatrix} 1 & \sqrt{\rho_{\text{HHP}}} \\ \sqrt{\rho_{\text{HHP}}} & 1 \end{pmatrix}.$$

If we denote $U_i = \Phi(X_i)$ for $i \in \{\text{H}, \text{HP}\}$, then $\mathbf{U} = (U_{\text{H}}, U_{\text{HP}}) \sim C_p^{Ga}$. If the probability that company i will survive by time T is $S_i(T; \boldsymbol{\beta})$, under the Gauss copula model, company i survives by time T once $\Phi(X_i) \leq S_i(T; \boldsymbol{\beta})$ or $X_i \leq \Phi^{-1}(S_i(T; \boldsymbol{\beta}))$. Considering (3.8), we could obtain that:

$$\zeta_i \leq \frac{\Phi^{-1}(S_i(T; \boldsymbol{\beta})) - \sqrt{\rho_i}V}{\sqrt{1 - \rho_i}}. \quad (3.9)$$

Thus, conditional on the value of V , the survival probability can be expressed as:

$$\bar{F}_{\tau_i|V}(T|v) = \mathbb{P} \left(\zeta_i \leq \frac{\Phi^{-1}(S_i(T; \boldsymbol{\beta})) - \sqrt{\rho_i}V}{\sqrt{1 - \rho_i}} \middle| V = v \right). \quad (3.10)$$

When we use one-factor Gauss copula model to price the credit risk, it is usually assumed that ρ_i equals ρ for all companies. Thus, in this thesis, we apply the exchangeable Gauss copula model with $\rho_i = \rho$.

Chapter 4

BCVA of K-forward

In this section, we mainly focus on calculating BCVA of K-forwards. We assume that a K-forward is written on the Canadian population aged from 50 to 89. There are two groups of potential traders: JP Morgan and New York Life, and JP Morgan and Prudential Financial. Gregory (2012) provides a general formula for BCVA based on the assumption that the default of the institution and the counterparty are independent and that the defaults can't happen at the same time for both parties. In this thesis, we will consider the correlation between two parties and use one-factor Gauss copula mentioned in the previous chapter. Then formula (1.2) becomes

$$\begin{aligned} \text{BCVA} = & (1 - R_{\text{HP}}) \mathbb{E} \left[\bar{F}_{\tau_{\text{H}}|V}(T|v) \int_0^T D(t) \cdot EE^+(t) \cdot f_{\tau_{\text{HP}}|V}(t|v) dt \right] \\ & - (1 - R_{\text{H}}) \mathbb{E} \left[\bar{F}_{\tau_{\text{HP}}|V}(T|v) \int_0^T D(t) \cdot EE^-(t) \cdot f_{\tau_{\text{H}}|V}(t|v) dt \right]. \quad (4.1) \end{aligned}$$

From (3.10) we know that for $i \in \{H, HP\}$,

$$\bar{F}_{\tau_i|V}(t|v) = \Phi \left(\frac{\Phi^{-1}(S_i(t; \boldsymbol{\beta})) - \sqrt{\rho}v}{\sqrt{1-\rho}} \right),$$

and thus

$$f_{\tau_i|V}(t|v) = -\phi \left(\frac{\Phi^{-1}(S_i(t; \boldsymbol{\beta})) - \sqrt{\rho}v}{\sqrt{1-\rho}} \right) \frac{S'_i(t; \boldsymbol{\beta})}{\sqrt{1-\rho} \phi(\Phi^{-1}(S_i(t; \boldsymbol{\beta})))} \quad (4.2)$$

where $\Phi(\cdot)$ and $\phi(\cdot)$ are the cdf and pdf of the standard normal distribution and $S_i(\cdot; \boldsymbol{\beta})$ is the survival probability for company i .

4.1 Expected risk exposures EE^+ and EE^-

In this section, we give the closed-form formulas for $EE^+(t)$ and $EE^-(t)$. From the LLCBD model (2.3), we have

$$\begin{aligned} \kappa_T &= \kappa_t + \Delta\kappa_{t+1} + \Delta\kappa_{t+2} + \cdots + \Delta\kappa_T \\ &= \kappa_t + (C_t + \xi_{t+1}) + (C_{t+1} + \xi_{t+2}) + \cdots + (C_{T-1} + \xi_T) \\ &= \kappa_t + (C_t + C_{t+1} + \cdots + C_{T-1}) + (\xi_{t+1} + \xi_{t+2} + \cdots + \xi_T) \\ &= \kappa_t + (T-t)C_t + v_{t+1} + (v_{t+1} + v_{t+2}) + \cdots + (v_{t+1} + v_{t+2} + \cdots + v_{T-1}) \\ &\quad + (\xi_{t+1} + \xi_{t+2} + \cdots + \xi_T). \end{aligned}$$

So

$$\begin{aligned} E(t) &= \mathbb{E} [\tilde{\kappa}_T - \kappa_T | \kappa_t, C_t] = \tilde{\kappa}_T - \mathbb{E} [\kappa_T | \kappa_t, C_t] = \tilde{\kappa}_T - \kappa_t - (T - t)C_t \\ &= - \sum_{j=1}^t [(T - j)v_j + \xi_j] \sim N(0, \sigma_t^2), \end{aligned}$$

where $\sigma_t^2 = t\sigma_\xi^2 + \sigma_v^2 [(T - 1)T(2T - 1) - (T - t - 1)(T - t)(2T - 2t - 1)] / 6$ and we use the fact that $\tilde{\kappa}_T = \kappa_0 + T \cdot C_0$. So $\mathbb{E}[E(t)] = 0$, which implies $EE^+(t) = \mathbb{E}[\max(E(t), 0)] = -\mathbb{E}[\min(E(t), 0)] = EE^-(t)$. Also,

$$EE^+(t) = \int_0^\infty \frac{x}{\sigma_t \sqrt{2\pi}} \exp \left\{ -\frac{x^2}{2\sigma_t^2} \right\} dx = \frac{\sigma_t}{\sqrt{2\pi}}. \quad (4.3)$$

4.2 Numeric Results

The detailed simulation procedure is shown in the following:

Step 1: Set the correlation ρ .

Step 2: Simulate 1,000,000 v 's from $N(0, 1)$.

Step 3: Calculate BCVA in (4.1) for each simulated v in Step 2 and calculate the average.

Step 4: Change the value of ρ , repeat Steps 1-3 to obtain the average BCVA for different ρ .

The numeric results of BCVA on K-forward is illustrated in Tables 4.1-4.3. In this case, we assume that $\rho = 0, 0.5, 0.95$ respectively and all results are measured in basis points (bpts):

Table 4.1: BCVA (in bpts) of K-forwards when $R = 0.37$ and $\rho = 0$

	$T = 15$		$T = 20$		$T = 25$	
	K1	K2	K1	K2	K1	K2
JPM-NYL	-0.23 (0.00)	-0.01 (0.00)	-12.28 (0.00)	-0.22 (0.00)	-18.46 (0.00)	-0.34 (0.00)
JPM-PF	-15.31 (0.00)	-0.22 (0.00)	-25.67 (0.00)	-0.41 (0.00)	-30.40 (0.00)	-0.50 (0.00)

Table 4.2: BCVA (in bpts) of K-forwards when $R = 0.37$ and $\rho = 0.5$

	$T = 15$		$T = 20$		$T = 25$	
	K1	K2	K1	K2	K1	K2
JPM-NYL	-0.28 ($4.62e^{-8}$)	-0.01 ($1.11e^{-9}$)	-11.00 ($1.32e^{-6}$)	-0.20 ($2.38e^{-8}$)	-16.57 ($1.95e^{-6}$)	-0.30 ($3.61e^{-8}$)
JPM-PF	-15.60 ($2.28e^{-6}$)	-0.23 ($3.20e^{-8}$)	-24.43 ($2.86e^{-6}$)	-0.39 ($4.50e^{-8}$)	-28.43 ($3.21e^{-6}$)	-0.47 ($5.35e^{-8}$)

Table 4.3: BCVA (in bpts) of K-forwards when $R = 0.37$ and $\rho = 0.95$

	$T = 15$		$T = 20$		$T = 25$	
	K1	K2	K1	K2	K1	K2
JPM-NYL	-0.34 ($1.91e^{-7}$)	-0.01 ($3.72e^{-9}$)	-8.78 ($3.84e^{-6}$)	-0.16 ($6.88e^{-8}$)	-12.57 ($5.61e^{-6}$)	-0.23 ($1.05e^{-7}$)
JPM-PF	-15.86 ($7.2e^{-6}$)	-0.25 ($1.16e^{-7}$)	-21.00 ($8.51e^{-6}$)	-0.35 ($1.44e^{-7}$)	-22.74 ($9.64e^{-6}$)	-0.39 ($1.71e^{-7}$)

According to results of BCVA in Tables 4.1–4.3, the most important difference between BCVA and CVA is that the sign in front of the counterparty credit risk valuation. When we use Canadian male aged from 50 to 89 as our reference population, for both of K1-forward and K2-forward, BCVA is negative for hedgers, whereas CVA must be non-negative. It indicates that the default risk valuation of

hedger is larger than the default valuation of hedge provider when they have the same recovery rate. Thus it is meaningful to calculate the BCVA when investors want to evaluate the credit risk of financial derivatives.

When we take an insight of the BCVA, we find that the absolute value of BCVA in K1-forward is obviously larger than the absolute value of BCVA in K2-forward. For example, in Table 4.2, when maturity is 25 years, the BCVA is -16.57 basis points for K1-forward, and -0.3 basis points for K2-forward. One reasonable explanation for this situation is that $\kappa^{(1)}$ contains more influence on the longevity risk than $\kappa^{(2)}$ contains. From definition of mortality indexes, $\kappa^{(1)}$ effects mortality rate at whole age, while $\kappa^{(2)}$ is the slope of the logit-transformed mortality curve and only influence mortality rate at certain ages. Also from Figure 2.1, we could observe that the fluctuation in $\kappa^{(1)}$ is larger than the fluctuation in $\kappa^{(2)}$. Therefore, $\kappa^{(1)}$ contains main longevity risk along with time.

Another finding in the BCVA is that hedger's and hedge provider's relative credit rating has significant influence on BCVA. For these three potential participants of K-forward, both JP Morgan and New York Life lie in the A-rating credit class, while Prudential Financial is in B-rating credit class. In Table 4.1 - 4.3, given the same maturity, correlation and type of K-forward, the absolute value of BCVA is larger for the group of JP Morgan and Prudential Financial than that for the group of JP Morgan and New York Life. It reflects the fact that investor in lower credit rating is more likely to default and therefore the value of default risk is also higher. In this thesis, both of New York Life's default valuation and Prudential Financial's valuation are higher than JP Morgan's, but Prudential Financial lies in

a lower credit rating class than New York Life and decrease BCVA further. That is the reason why BCVA for the group of JP Morgan and Prudential Financial is lower.

Additionally, in this thesis, we incorporate the correlation of two traders into the BCVA calculation. According to the sensitive test on ρ , we could find that the correlation could influence the BCVA value. In short term, the BCVA decreases as the correlation between two investors increases. However, when it comes to long term, the rise in the correlation increases the BCVA. For instance, given that maturity is 25 years and participants are JP Morgan and New York Life, if we increase ρ from 0 to 0.5, the BCVA increase 10.24% for K1-forward and 11.76% for K2-forward. Given the same condition, if we increase ρ from 0.5 to 0.95, the BCVA increase 24.14% for K1-forward and 23.33% for K2-forward. The changes on BCVA are evident. As a result, it is meaningful to consider the correlation when we evaluate the counterparty credit risk.

Chapter 5

Concluding remarks and future study

5.1 Thesis summary

In this thesis, we propose a baseline framework to calculate BCVA in K-forward. We use LLCBD mortality model to obtain the mortality indexes. LLCBD mortality model provides better estimations than the original two-factor CBD mortality model. Relying on the mortality model, future risk exposures can be estimated. Then, we consider the default probability of each potential traders. After comparing the structural model and the reduced-form model, we decide to use the reduced-form model to construct the marginal risk-neutral default probability. The optimized parameters for hazard rate are calibrated by matching bond's market price with its "dirty price" and minimizing the average absolute error. In the calculation process of BCVA, there are two participants in the transaction of K-forwards. In real financial market, the performance of one company may influence that of the other. To include such effect, we select copula to include the correlation effect into

the general BCVA model. For simplicity, one-factor Gaussian copula is applied to obtain the joint default probability.

The main contributions of this thesis are summarized as follows.

- (1) We propose a general method which to price BCVA for longevity-linked security. Unlike the UCVA in many literatures, this method reflects the bilateral nature of the counterparty risk. It makes the valuation more reasonable and accurate, because it is almost impossible to suppose that hedger will never bankruptcy. Moreover, according to the empirical results, the value of BCVA is significantly different from 0 in long term. It indicates that it is meaningful to calculate BCVA for the valuation of counterparty risk, especially for long-term financial derivatives.
- (2) We compare two different mortality models. Considering the reference population, we choose LLCBD model which includes the stochastic nature of the drift and performs better in the forecasting process. Thus, we are able to obtain more reliable risk exposures.
- (3) We use copula to describe the default correlation between two participants. This is different from previous literatures which usually assume that there is no correlation between the defaults of the two traders. However, this assumption is not realistic when we consider the real financial market. After applying one-factor Gauss copula to BCVA computation, we are able to observe the default correlation effect on BCVA. This method is more realistic and applies to more general situations.

- (4) Based on the empirical results, we find that the default correlation, the relative credit rating, maturity years and type of K-forward do have influence on the value of BCVA. Knowing the influential factors of BCVA could help us to precisely evaluate counterparty risk.

5.2 Future Research

In this paper, we set the recovery rate as a constant number. However, in financial market, the recovery rate is random and could be influenced by the company's performance. When we set a constant recovery rate, we ignore the possible recovery risk and reduce the accuracy of BCVA. In the future, we could find another model which could take into account random recovery risk in the price of counterparty risk. One simple way is to use a piecewise random recovery rate which depends on default severity. Or it is better to include a continuous random recovery rate. Additionally, in this thesis, we only applied the reduced-form model to get the default probability. In the next step, we could also calculate the default probability via a structural model and compare the results. Then, it is possible to figure out if there exists severe model risk in the methodology of pricing the counterparty risks.

Another issue which need further study is correlation ρ . Although we consider the dependency on the defaults of two traders, we set the correlation arbitrarily. It is necessary to find a proper correlation coefficient to describe the dependency between two parties of K-forward at time t . One possible solution is to use asset correlation to replace the default correlation. Or we could try to find a set of first-

to-default swap which contains the target institutions and use the market price to deduce ρ for the potential traders.

Bibliography

- Bielecki, T., & Rutkowski, M. (2001). *Credit risk: modeling, valuation and hedging*. Berlin, Heidelberg: Springer Finance.
- Blake, D., Cairns, A., Coughlan, G., Dowd, K., & MacMinn, R. (2013). The new life market. *Journal of Risk and Insurance*, 80(3), 501–558.
- Bluhm, C., Overbeck, L., & Wagner, C. (2010). *Introduction to Credit Risk Modeling*. Boca Raton, Florida: CRC Press.
- Brigo, D., Capponi, A., Pallavicini, A., & Papatheodorou, V. (2011). Collateral Margining in Arbitrage-Free Counterparty Valuation Adjustment including Re-Hypotecation and Netting (Working Paper No. 1697577043). Retrived from <http://uml.idm.oclc.org/login?url=https://search-proquest-com.uml.idm.oclc.org/docview/1697577043?accountid=14569>
- Brigo, D., & Capponi, A. (2010). Bilateral counterparty risk with application to CDSs. *Risk*, 23(3), 85-90.
- Cairns, A., Blake., D., & Dowd, K. (2006). A two-factor model for stochastic

- mortality with parameter uncertainty: theory and calibration. *Journal of Risk and Insurance*, 73(4), 687–718.
- Chan, W., Li, J., & Li, J. (2014). The CBD mortality indexes: modeling and applications. *North American Actuarial Journal*, 18(1), 38–58.
- Cox, S. H., & Pedersen, H. W. (2000). Catastrophe risk bonds. *North American Actuarial Journal*, 4(4), 56-82.
- Dowd, K., Cairns, A., Blake, D., Coughlan, G., Epstein, D., & Khalaf-Allah, M. (2010). Backtesting stochastic mortality models: an ex post evaluation of multiperiod-ahead density forecasts. *North American Actuarial Journal*, 14(3), 281–298.
- Duan, J. C., Sun, J., & Wang, T. (2012). Multiperiod corporate default prediction – a forward intensity approach. *Journal of Econometrics*, 170(1), 191–209.
- Duffie, D., & Huang, M. (1996). Swap Rates and Credit Quality. *Journal of Finance*. 51(3), 921-949.
- Gallp, A. (2006). Mortality improvements and evolution of life expectancies. Paper presented at the Seminar on Demographic, Economic and Investment Perspectives for Canada, Office of the Superintendent of Financial Institutions Canada.
- Gregory, J. (2015). *The XVA Challenge: Counterparty Credit Risk, Funding, Collateral and Capital*. Hoboken, New Jersey: John Wiley & Sons.

- Hao, X., Li, X., & Shimizu, Y. (2013). Finite-time survival probability and credit default swaps pricing under geometric Levy markets. *Insurance: Mathematics and Economics*, 53(1), 14-23.
- Hao, X., Liang, C., & Wei, L. (2017). Evaluation of credit value adjustment in K-forward. *Insurance: Mathematics and Economics*, 76, 95-103.
- Hari, N., De Waegenaere, A., Melenberg, B., & Nijman, T. E. (2008). Longevity risk in portfolios of pension annuities. *Insurance: Mathematics and Economics*, 42(2), 505-519.
- Holmes, E. E. (2013). Derivation of an EM algorithm for constrained and unconstrained multivariate autoregressive state-space (MARSS) models. Retrieved from <https://arxiv.org/abs/1302.3919>.
- Hull, J. (2014). *Options, Futures, and Other Derivatives*. London: Pearson Education.
- Human Mortality Database. (2017). University of California, Berkeley, USA, and Max Planck Institute for Demographic Research, Germany. Available at www.mortality.org.
- Imhof, H. P. (1961). Computing the distribution of quadratic forms in normal variables. *Biometrika*, 48(3/4), 419-426.
- Jarrow, R. A., & Turnbull, S. (1995). Pricing derivatives on financial securities subject to credit risk. *Journal of Finance*, 50(1), 53-85.

- Jarrow, R. A. (2011). Credit market equilibrium theory and evidence: Revisiting the structural versus reduced form credit risk model debate. *Finance Research Letters*, 8(1), 2-7.
- Lando, D., & Mortensen, A. (2005). Revisiting the slope of the credit spread curve. *Journal of Investment Management*, 3(4), 1-27.
- Liu, Y., & Li, J. (2016). The locally linear Cairns–Blake–Dowd model: a note on delta–nuga hedging of longevity risk. *ASTIN Bulletin*, 47(1), 79–151.
- McNeil, A. F., Frey, R. & Embrechts, P. (2015) *Quantitative Risk Management*. Princeton, New Jersey: Princeton University Press.
- Merton, R. C. (1974). On the pricing of corporate debt: the risk structure of interest rates. *Journal of Finance*, 29(2), 449-470.
- Nelson, C.R.; Siegel, A.F. (1987). Parsimonious modeling of yield curves. *Journal of Business*, 60(4), 473–489.
- Nyblom, J., & Mäkeläinen T. (1983) Comparisons of tests for the presence of random walk coefficients in a simple linear model. *Journal of the American Statistical Association*, 78(384), 856-864.
- Tan, C., Li, J., Li, J., & Balasooriya, U. (2014). Parametric mortality indexes: From index construction to hedging strategies. *Insurance: Mathematics and Economics*, 59, 285–299.
- Vaupel, J. W. (1997). The remarkable improvements in survival at older ages.

Philosophical transactions of the Royal Society B: Biological Sciences, 352(1363),
1799-1804.